Nonelectrolyte Permeability, Sodium Influx, Electrical Potentials, and Axolemma Ultrastructure in Squid Axons of Various Diameters

RAIMUNDO VILLEGAS, GLORIA M. VILLEGAS, REINALDO DIPOLO, and JORGE VILLEGAS

From the Centro de Biofísica y Bioquímica, Instituto Venezolano de Investigaciones Científicas (IVIC), Apartado 1827, Caracas, Venezuela

ABSTRACT The penetration of ^{14}C-labeled ethylene glycol, erythritol, mannitol, and sucrose was measured in giant axons of various diameters isolated from the hindmost stellar nerves of *Doryteuthis plei* squid. Axon diameter depends mainly on the age of the squid. The influx of ^{22}Na, some electrical properties, and the ultrastructure of the axolemma were also studied. The results confirm our previous observation that in medium sized axons of *D. plei* stimulation causes an increase in the permeability to the penetration of erythritol, mannitol, and sucrose. They also demonstrate that the magnitude of the increase in the penetration of these probing molecules diminishes progressively as the axon diameter increases. The diminution in permeability may be due to a reduction in size of the pathways used by nonelectrolytes to enter the axon. No effect of stimulation on the ethylene glycol permeability is observed. The sodium influx and electrical properties are independent of axon size. The ultrastructural study shows that the axolemma thickness increases with axon diameter. The present experiments indicate that the nonelectrolyte permeability of stimulated axons depends on nerve fiber properties related to axon diameter and on the size of the hydrophilic nonelectrolyte probe.

In giant axons of the squid, *Doryteuthis plei*, of about 300 μ diameter or less (also named medium sized axons in the present work) stimulation causes a reversible increase in the permeability to the penetration of erythritol, mannitol, and sucrose (1). This increase in nonelectrolyte permeability was not observed by Hodgkin and Martin (cited in reference 1), Mullins, (2), and Hidalgo and Latorre (3) in axons with larger diameters from other squid species.

The present work was carried out to investigate whether these controversial

results could be due to variations in nerve fiber properties related to axon diameter. Since for all experiments the paired giant axons from the two hindmost stellar nerves of *D. plei* were used, the diameter of the axons depends mainly on the age of the squid.

The results of the present work indicated that the entry of nonelectrolytes into stimulated axons depends on nerve fiber properties related to axon diameter and on the size of the hydrophilic nonelectrolyte probe.

EXPERIMENTAL METHOD

Since the methods used to study the nonelectrolyte permeabilities, sodium influx, electrical properties, and ultrastructure have been already described (see references 1, 4, and 5), only an outline of the procedures is given in the following paragraphs. All experiments were carried out at 22–23°C.

General Procedure

Living squid, *D. plei*, of different sizes were used. The pair of giant axons from the two hindmost stellar nerves of the mantle were isolated in about 10 min. Most of the small fibers and endoneurium were removed during the isolation procedure. Immediately, the axons were equilibrated for 5 min in artificial seawater while the lengths and diameters were measured.

The composition of the artificial seawater, in mmoles per liter, was as follows: NaCl, 442; KCl, 10; $CaCl_2$, 11; $MgCl_2$, 53; $NaHCO_3$, 2.5 (6).

Nonelectrolyte Permeability and Sodium Influx

The axon pairs were transferred to seawater baths containing either one of the ^{14}C-labeled nonelectrolytes or ^{22}Na in order to measure the nonelectrolyte permeability and sodium influx. The baths containing radioactive nonelectrolytes were prepared by adding to artifical seawater one of the following ^{14}C-labeled solutes: (*a*) 6.2 mmoles of ethylene glycol per liter, specific activity, 1.70 mCi per mmole; (*b*) 3.3 mmoles of erythritol per liter, specific activity, 3.00 mCi per mmole; (*c*) 4.7 or 18.0 mmoles of mannitol per liter, specific activities, 1.10 and 1.38 mCi per mmole, respectively; (*d*) 2.0 or 3.2 mmoles of sucrose per liter, specific activities, 3.02 and 3.09 mCi per mmole, respectively. The ^{22}Na-labeled baths were prepared by adding 0.90–1.30 μCi of ^{22}Na per ml.

Both axons of each pair were immersed in approximately 5 ml of the same radioactive bath for the same period in two separate holders, one axon at rest and the other stimulated at 5, 25, or 50 stimuli per sec (see Tables I–IV). The holders had four platinum electrodes above the seawater level, two for stimulation and two for recording. A fifth platinum electrode immersed in the bath was used to ground the preparation. About 3 mm at both ends of the nerve fiber were placed on the electrodes and were kept wet with hanging drops of radioactive seawater. The time of immersion for each axon pair in the radioactive solutions was 3, 5, or 10 min. The axons were stimulated for 1 min less than the immersion period in the radioactive bath. At the end of the immersion period the fiber was taken out, soaked for about 15 or 30 sec in non-

radioactive seawater, blotted with filter paper, cut 5 mm from one end, and the axoplasm extruded. The drop of extruded axoplasm was collected on filter paper, weighed, and finally transferred to a Tri-Carb glass flask for ^{14}C counting or to a glass test tube for ^{22}Na measurement. Due to the large ethylene glycol permeability of the axons, the values of this nonelectrolyte were corrected, taking into account the time of soaking in the nonradioactive seawater. The results for the nonelectrolytes are expressed in permeability units of cm/sec and for sodium in moles/$cm^2 \cdot$sec. The values are given as mean $\pm$ SEM.

Electrical Potentials

In order to measure the electrical potential differences across the axolemma, at rest and during the action potential, conventional intracellular recording procedures were used (5). The maximum rates of rise and fall of membrane voltage during the action potential were simultaneously measured by electrical differentiation using the method of Hodgkin and Katz (6). The time constant of the condenser and resistance used for differentiating was about 13 μsec.

Ultrastructure

In order to study the axon membrane ultrastructure, the nerve fibers were fixed by immersion in an ice-cold, veronal-buffered, OsO_4 solution in artificial seawater at pH 7.9. After 1 hr fixation the samples were dehydrated in a series of acetone solutions and then embedded in Epon 812. Ultrathin sections were doubly stained with uranyl acetate and lead citrate and examined in a Siemens Elmiskop 1 A electron microscope, at a magnification of 70,000, tested each time with a carbon grating replica (54,800 lines/inch) and a resolution of 4 A, measured by the point-to-point separation method. Measurements of the axolemma thickness on the electron micrograph negative plates were made with a Nikon (Nippon Kogaku KK, Tokyo, Japan) profile projector, model 6 C. A total of 27 measurements of the axolemma obtained from 6 to 13 different electron micrographs was made for each axon. Only those regions of the axolemma showing a clear and definite three-layered pattern were measured, in order to avoid the uncertainties in thickness caused by tangential sections of the membrane. The thickness of the leaflets forming the three-layered pattern of the axolemma was measured separately.

RESULTS AND DISCUSSION

Nonelectrolyte Permeabilities

93 pairs of nerve fibers were utilized for the determination of permeabilities of resting and stimulated giant axons of different diameters to the penetration of ethylene glycol, erythritol, mannitol, and sucrose.

Table I summarizes the results of the experiments with ethylene glycol. It is seen that the entry of this nonelectrolyte is independent of axon diameter and is the same in resting and stimulated axons. A slight increase of permeability during activity was previously observed in paired axons, taking into consideration the frequency of stimulation (7). However, as shown in Table I,

there is no difference when the permeability values of groups of axons are considered.

Tables II–IV and Figs. 1–3 show the results of the erythritol, mannitol, and sucrose experiments. They indicate that the resting permeabilities are independent of axon diameter and are increased by stimulation in medium sized axons,[1] the magnitude of the increment diminishing progressively as the axon diameter increases. The increased nonelectrolyte flux during a period of activity may actually be due to other factors than a permeability change. For example, increased solvent or electrolyte drag might improve the stirring of the compartment outside the axolemma or increase the transport through unaltered nonelectrolyte pores. In this paper, however, the increase in flux is assumed to be due to an increase in permeability. It is further assumed that

TABLE I

PENETRATION OF ETHYLENE GLYCOL IN PAIRED AXONS, ONE AT REST AND THE OTHER STIMULATED

Temperature 21–23°C

	Axon a Rest		Axon b Stimulated (50 times/sec)	
No. of axon pairs	Diameter	Permeability	Diameter	Permeability
	μ	10^{-7} cm/sec	μ	10^{-7} cm/sec
5	224±5	220±34	244±6	232±38
6	281±13	199±35	277±11	213±23
7	318±14	229±41	323±15	240±29
6	355±10	217±64	371±12	220±56

Values are mean ± SEM.

nonelectrolyte permeability increases for 1 msec per impulse. Under these assumptions the permeabilities during activity of medium sized axons, expressed as 10^{-7} cm/sec, are 76 for erythritol, 79 for mannitol, and 42 for sucrose. The corresponding resting permeabilities in the same units are 1.6 for erythritol, 1.1 for mannitol, and 0.9 for sucrose. It should be noticed that the permeability measured in stimulated axons may be an apparent permeability coefficient because of the coexistence of other fluxes (ions and water) that can affect the entrance of the nonelectrolytes.

[1] Control experiments carried out with erythritol in 12 pairs of medium sized axons have shown that the ratio of the permeabilities of paired resting axons is 1.0 ± 0.1 (mean ± SEM) and that of the increased permeabilities in paired stimulated axons is 0.97 ± 0.08. These ratios indicate that the resting permeability is the same in both axons of the pairs and that the increase in permeability caused by stimulation is the same in both axons of a pair. Evidence has also been presented which indicates that the change in permeability observed in stimulated axons is reversible and not due to a permanent alteration of the axolemma structure (1). It has been shown by paper radiochromatography that these ^{14}C-labeled nonelectrolyte molecules remain unaltered after passing the transneural barriers of the resting and stimulated nerve fibers.

It may be observed from the lines representing the logarithm of the permeability during activity as a function of axon diameter (Figs. 1–3), that erythritol, mannitol, and sucrose permeabilities also depend on the size of the corresponding nonelectrolyte molecule. The slopes of these lines, in 10^2 cm^{-1}, are 2.2 for erythritol, 2.9 for mannitol, and 3.6 for sucrose. The ratios between

TABLE II

PENETRATION OF ERYTHRITOL IN PAIRED AXONS, ONE AT REST AND THE OTHER STIMULATED

Temperature 21–23°C

Axon a at rest		Axon b stimulated			Permeability ratio	Calculated permeability
Diameter	Permeability	Diameter	Stimuli/sec	Permeability	Axon b: Axon a	during activity*
μ	10^{-7} cm/sec	μ		10^{-7} cm/sec		10^{-7} cm/sec
226	1.5	222	25	3.5	2.3	84
231	2.1	231	25	4.2	2.0	92
230	1.0	231	50	2.5	2.5	32
235	1.9	232	25	4.6	2.4	112
235	1.8	235	50	6.2	3.4	95
254	2.1	250	25	3.9	1.9	80
253	2.9	253	25	5.2	1.8	102
259	3.1	264	25	5.9	1.9	121
268	1.7	264	50	6.9	4.1	111
267	2.6	267	50	5.6	2.2	65
274	2.8	274	25	2.9	1.0	8
278	3.8	281	25	4.2	1.1	33
281	1.0	283	25	3.6	3.6	35
277	2.8	296	50	3.3	1.2	14
284	1.5	296	25	2.0	1.3	21
296	2.4	292	50	4.8	2.0	53
300	1.0	306	50	1.7	1.7	15
324	1.9	330	50	2.3	1.2	11
327	1.8	332	25	2.7	1.5	38
330	1.8	336	25	1.8	1.0	2
342	0.9	342	50	1.5	1.7	13
348	1.9	342	50	1.6	0.8	2
353	1.4	349	25	1.4	1.0	1
369	1.6	345	25	1.6	1.0	2
375	1.8	375	50	2.7	1.5	22
381	2.0	378	50	2.2	1.1	6

* Permeability during activity calculated from the data of axons a and b and the frequency of stimulation. The permeability change per impulse is considered to last 1 msec.

these slopes are similar to those between the molecular radii of erythritol, mannitol, and sucrose. The radii of these molecules, as obtained from constructed molecular models, are 3.1, 4.0, and 4.5 A, respectively. It should be noted also that the lines representing the permeabilities during activity intersect with those of the resting permeabilities at axon diameters of about 410 μ for erythritol, 390 μ for mannitol, and 350 μ for sucrose.

The decline with axon diameter of the permeabilities during activity could be due to a progressive reduction in the size of the pathways used by the non-electrolytes to move through the axolemma. On the other hand, the different slopes and intersections of the lines for erythritol, mannitol, and sucrose should depend on the fact that a narrow pathway has different effective areas according to the size of the probing molecule.

TABLE III

PENETRATION OF MANNITOL IN PAIRED AXONS, ONE AT REST AND THE OTHER STIMULATED

Temperature 21–23°C

Axon a at rest		Axon b stimulated			Permeability ratio	Calculated permeability
Diameter	Permeability	Diameter	Stimuli/sec	Permeability	Axon b : axon a	during activity*
μ	10^{-7} cm/sec	μ		10^{-7} cm/sec		10^{-7} cm/sec
216	1.7	221	25	5.0	2.9	143
228	0.9	228	25	3.0	3.3	88
231	1.7	231	25	4.0	2.4	97
247	0.5	246	50	2.0	2.0	32
258	1.9	257	50	6.5	3.4	99
257	1.1	260	5	1.4	1.8	63
259	2.7	269	25	4.4	1.6	76
264	1.0	264	25	2.2	2.2	50
274	3.5	274	25	5.0	1.4	67
278	2.1	274	25	2.7	1.3	25
275	1.1	281	25	1.7	1.5	25
278	0.7	278	50	1.6	2.3	19
284	1.4	280	50	1.7	1.2	8
282	3.8	284	25	6.7	1.8	129
298	0.7	287	50	1.1	1.6	8
303	0.5	307	50	1.1	2.2	3
321	1.0	315	50	1.5	1.5	11
328	0.5	323	50	0.4	0.8	1
330	1.3	330	50	2.0	1.5	17
333	1.0	327	50	1.1	1.1	2
363	0.9	361	50	0.9	1.0	1
375	1.8	381	50	1.9	1.1	4

* Permeability during activity calculated from the data of axons a and b and the frequency of stimulation. The permeability change per impulse is considered to last 1 msec.

Sodium Influx

10 pairs of nerve fibers were utilized for measurements of sodium influx in resting and stimulated axons. There is no apparent relationship between sodium influx and axon diameter. The values of the influx in resting and stimulated axons of different diameters were similar to those previously reported (1).

The average sodium influx at rest is 148 ± 11 pmoles/cm²·sec. It should be

noted that the magnitudes of the influx and efflux of sodium in resting *D. plei* axons (1) are greater than those of the axons of *Sepia officinalis*, *Loligo pealei* and *Loligo forbesi* (8–10). This should be due to species differences. The temperature of the water in which *D. plei* lives is from 25° to 28°C.

The average sodium influx during activity is 5.0 ± 0.2 pmoles/cm²·impulse. The experimental values for 10 pairs of axons of different diameters are shown

TABLE IV

PENETRATION OF SUCROSE IN PAIRED AXONS, ONE AT REST AND THE OTHER STIMULATED

Temperature 21–23°C

Axon a at rest		Axon b stimulated			Permeability ratio	Calculated permeability
Diameter	Permeability	Diameter	Stimuli/sec	Permeability	Axon b : axon a	during activity*
μ	10^{-7} cm/sec	μ		10^{-7} cm/sec		10^{-7} cm/sec
232	1.0	231	25	2.9	2.9	80
242	0.4	238	50	1.1	2.8	15
242	0.6	240	50	1.2	2.0	13
246	1.6	245	25	4.0	2.5	101
244	1.2	248	25	3.2	2.7	84
252	1.2	252	50	2.7	2.3	37
260	0.7	256	50	1.4	2.0	15
260	0.6	261	25	2.0	3.3	59
270	1.0	269	25	1.3	1.3	13
278	1.0	274	25	1.3	1.3	13
282	0.6	282	50	1.1	1.8	11
288	0.7	292	25	0.9	1.3	8
315	1.2	309	25	1.2	1.0	1
324	1.0	327	25	0.6	0.6	1
327	0.9	327	50	0.7	0.8	1
345	1.2	339	25	1.4	1.2	8
336	0.6	348	50	0.6	1.0	1
345	1.4	357	25	1.4	1.0	1
360	1.0	378	50	1.0	1.0	1
378	0.9	366	50	1.2	1.3	6
379	0.9	384	50	0.8	0.9	1

* Permeability during activity calculated from the data of axons a and b and the frequency of stimulation. The permeability change per impulse is considered to last 1 msec.

in Fig. 4. The sodium influx per impulse is about equal to that found in other squid species (11). Each value shown in Fig. 4 for the influx per impulse was calculated by subtracting the value for the stimulated axon from that of the paired resting axon and then dividing the net increase by the frequency of stimulation.

Electrical Potentials

14 nerve fibers were utilized to investigate the possibility of a relationship between the electrical potential differences across the axolemma at rest or during

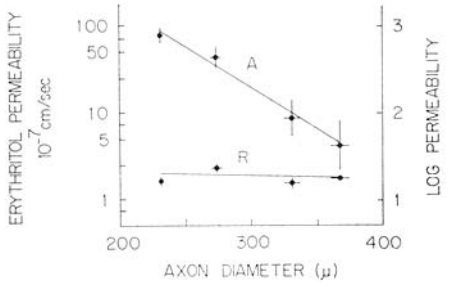

FIGURE 1

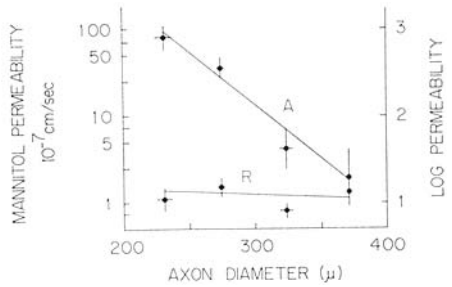

FIGURE 2

FIGURE 1. Permeability to the penetration of erythritol at rest (*R*) and during activity (*A*), represented as functions of axon diameter. Each value corresponds to the mean ± 1 SEM of the permeability and axon diameter. The data in Table II were grouped according to intervals of 50 μ in axon diameter. Temperature, 21–23°C.

FIGURE 2. Permeability to the penetration of mannitol at rest (*R*) and during activity (*A*), represented as functions of axon diameter. Each value corresponds to the mean ± 1 SEM of the permeability and axon diameter. The data in Table III were grouped according to intervals of 50 μ in axon diameter. Temperature, 21–23°C.

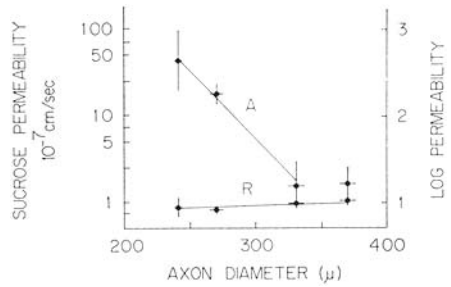

FIGURE 3. Permeability to the penetration of sucrose at rest (*R*) and during activity (*A*), represented as functions of axon diameter. Each value corresponds to the mean ± 1 SEM of the permeability and axon diameter. The data in Table IV were grouped according to intervals of 50 μ in axon diameter. Temperature, 21–23°C.

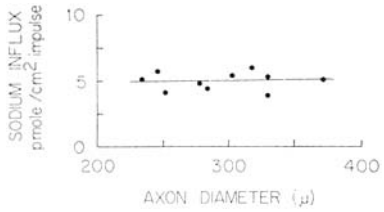

FIGURE 4. Sodium influx per impulse represented as a function of axon diameter. The values were calculated from experimental results obtained in paired axons, one at rest and the other stimulated. Temperature, 21–23°C.

the action potential and the axon diameter. Simultaneous determinations of the rates of membrane potential change during the rise and fall of the action potential were also made. As shown in Figs. 5 and 6, the values were found to be independent of axon diameter.

Axolemma Ultrastructure

The electron microscopic study of the axolemma reveals that this membrane presents, in addition to the regions of the three-layered pattern considered characteristic of plasma membranes, certain zones formed by globular repeating units (4). The three-layered substructure is formed by a clear middle layer bordered by two dark layers. In the axolemma, as in most of the plasma membranes (12), the inner dark layer is thicker than the outer layer. Furthermore, local thickenings of the dark layer at the axoplasmic side, rather regularly spaced along the axolemma, are observed.

The axolemma thickness, taken as an index of variation in membrane structure, was measured in 19 nerve fibers. As shown in Fig. 7, it increases exponentially from about 93 to 104 A for axons augmenting from 200 to more

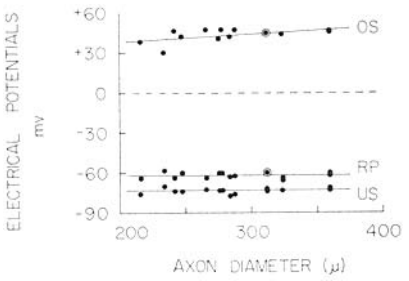

FIGURE 5

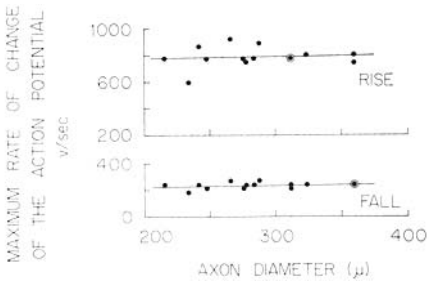

FIGURE 6

FIGURE 5. The axon electrical potentials represented as a function of axon diameter. The resting potential (*RP*), as well as the overshoot (*OS*) and the undershoot (*US*) of the action potential is shown. Temperature, 21–23°C.

FIGURE 6 The maximum rates of change of the rising and falling phases of the action potential are represented as functions of axon diameter. Temperature, 21–23°C.

than 400 μ in diameter. As shown in Fig. 8, independent measurements of the three membrane leaflets indicate that the differences in total thickness appear to be due to variations in the outer and inner dark layers of the axolemma. Fig. 9 shows electron micrographs of the axon–Schwann cell boundary in giant axons with diameters between 228 and 430 μ. They show that the axolemma of large axons displays an over-all increase in electron density as compared to that of the axolemma of small axons and Schwann cell plasma membranes.

Histochemical reactions for demonstrating polysaccharides by electron microscopy have also shown that the accumulation of positive material at the axolemma external surface (axon–Schwann cell space), Schwan cell channels, and basement membrane is more pronounced around axons with diameters of about 400 μ than in those of approximately 200 μ (see reference 4).

These results indicate that the increase in axon diameter is accompanied by changes in the axolemma and the extracellular material. Although these changes may not be directly related to the modifications of the nonelectrolyte

permeabilities, they suggest that the variations in the entry of the nonelectrolytes could be due to a structural change in the nerve fibers.

Nonelectrolyte Permeability, Diffusion Barriers, and Axon Diameter

The main barriers at the surface of a nerve fiber of the squid, *D. plei*, are formed by (*a*) the axolemma which may be operationally described as a mem-

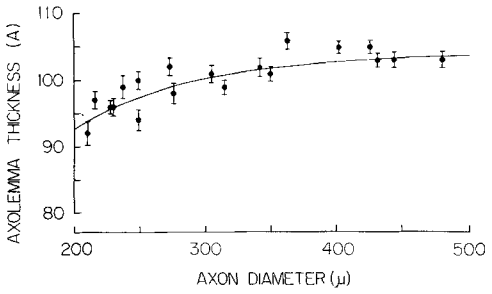

FIGURE 7. Total thickness of the axolemma represented as a function of axon diameter.

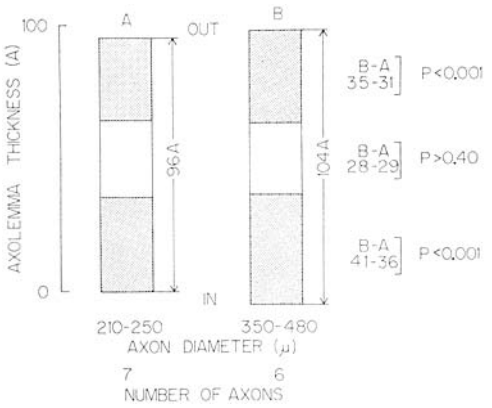

FIGURE 8. The total thickness of the axolemma and of each of the three leaflets making the membrane three-layered pattern for two different groups of axons. One group is formed by axons with diameters between 210 and 250 μ and the other by axons with diameters between 350 and 480 μ.

brane 80 A thick perforated by pores with an effective radius of 4-5 A in the resting axons, and (*b*) the Schwann cell layer crossed by 60 A wide slit channels with a length of 4–5 μ, connecting the extracellular space with the 80 A wide axolemma-Schwann cell space (13). The area occupied by the slit channels in 1 cm^2 of Schwann layer surface is some 20 times larger than the one occupied by the pores in 1 cm^2 of axolemma.[2]

[2] Calculated from Bruzual, I. B., and R. Villegas. Unpublished results.

The restriction offered by each barrier to the passage of a nonelectrolyte depends critically on the ratio of the area for diffusion to the length of the pathways crossing the barrier and on the size of the probing molecule. Thus, the restriction to the passage of the molecules offered by the channels crossing the Schwann cell layer is mainly due to their length, and that offered by the pores in the axolemma, to their small radius (13).

If a molecule present in the bathing medium has to penetrate inside the axon, it must pass through the periaxonal layers and the axolemma. Therefore, its rate of penetration will depend on the relative permeabilities of these barriers. In order to estimate the role played by each barrier during activity, it can be assumed that the permeability of the periaxonal layers remains constant and only that of the axolemma changes. Thus, if during activity the restriction to the passage of a given molecule at the axolemma is much less than that at the Schwann layer, the apparent transneural permeability during activity could be close to that of the Schwann cell layer.

Using the values of the effective areas for diffusion per unit path length for the Schwann cell layer and the axolemma, respectively, that can be calculated according to the size of the probing molecule (see reference 13), it may be estimated that in medium sized axons stimulated 100 times per sec (changes at the axolemma during 10% of the time), the increase in transneural permeability for hydrophilic molecules with radii of the order of 2 A should be less than 1.2 times the resting transneural permeability. This increase might be masked by the experimental errors. This conclusion is compatible with the results obtained with ethylene glycol, which has a radius of 2.2 A.

As the radius of the nonelectrolyte molecule increases to 3 A or more,[3] the restriction at the axolemma to the penetration of the molecule becomes important. Thus, a change at this barrier during activity will produce a significant increase in the apparent transneural permeability. This could be the case with erythritol, mannitol, and sucrose in medium sized axons. On the other hand, the results obtained with the same molecules in large axons indicate that when the size of the axon increases there is a diminution of the increment in permeability caused by stimulation. Since the ultrastructural studies have shown that the increase in axon diameter is accompanied by changes in the axolemma and periaxonal constituents, it might be suggested, following Mullins (2), that differences in permeability between stimulated axons of various diameters could be due to slight differences in the structure of the pathways or pores used by the nonelectrolytes to cross the axolemma during activity.

Thus, the increase in nonelectrolyte permeability caused by stimulation will depend on two main factors: nerve fiber properties related to axon diameter and size of the hydrophilic nonelectrolyte probe. To date, the increase has

[3] For hydrophilic nonelectrolyte molecules with radii larger than a certain critical value, which makes them impermeant to the resting and active axolemma, a change in permeability cannot exist.

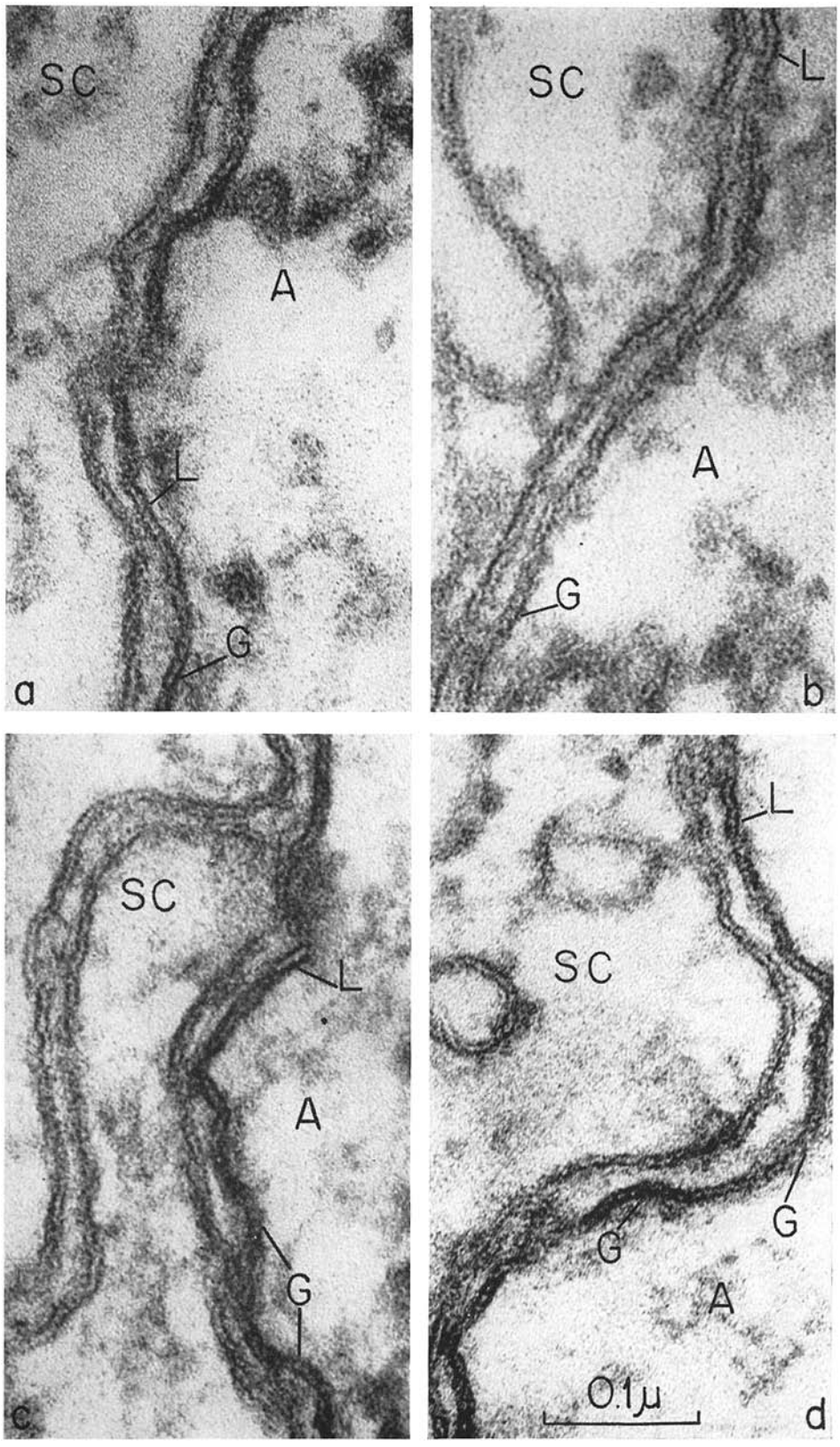
SC
A
L
G
a
SC
L
A
G
b
SC
L
A
G
c
L
SC
G
G
A
0.1μ
d

been observed using hydrophilic nonelectrolytes with 3–4.5 A radius and axons of about 300 μ diameter. In the squid, *D. plei*, axons of these sizes correspond to young animals. It should be noted that our results in large axons are in agreement with those obtained in large axons of other squid species by Hodgkin and Martin (cited in reference 1), Mullins (2), and Hidalgo and Latorre (3).

APPENDIX I

Nonelectrolyte–Sodium Coupling and Uncoupling

Erythritol experiments previously reported have shown that the nonelectrolyte permeability increase caused by stimulation in medium sized axons depends on external sodium concentration (1). We suggested (see reference 1) that this may be due (*a*) to a drag effect (coupling) on the nonelectrolyte molecules of the sodium ions which enter the axon during activity, since sodium influx also depends on the external sodium concentration, or (*b*) to independent effects of the sodium concentration on sodium influx and the nonelectrolyte pathways. The nonelectrolyte-sodium relationship is only apparent in stimulated axons, since experiments carried out in resting axons indicated that when the external sodium concentration is diminished, the erythritol penetration remains unchanged and the sodium influx decreases. Those results are summarized in Fig. 10. The data are taken from Tables V and VI of reference 1.

Since the increase in erythritol, mannitol, and sucrose permeabilities during activity gradually declines with increasing axon diameter and the extra sodium influx remains unchanged, we propose that if the drag effect exists, it is somehow dependent on axon diameter.

The proposed drag effect or coupling can be described by the following equations, if a linear relationship is assumed between the forces and the fluxes of sodium, J_e, and the nonelectrolyte, J_n :

$$J_n = L_{nn}X_n + L_{ne}X_e ;$$
$$J_e = L_{en}X_n + L_{ee}X_e ,$$

in which X_n and X_e are the driving forces of the nonelectrolyte and the electrolyte respectively; L_{nn} and L_{ee} are the direct coefficients, and L_{ne} and L_{en} are the respective cross-coefficients.

As a first approximation, it may be considered that at the nonelectrolyte concentrations used in our experiments, $L_{en}X_n$ is very much less than $L_{ee}X_e$. Solving for J_n , the following relation is obtained

$$J_n = L_{nn}X_n + (L_{ne}/L_{ee})J_e .$$

FIGURE 9. Electron micrographs of squid giant nerve fibers showing the axon (*A*)-Schwann cell (*SC*) boundary of axons with diameters of (*a*) 228 μ, (*b*) 240 μ, (*c*) 402 μ, and (*d*) 430 μ. The axolemma displays the three-layered (*L*) and the globular (*G*) substructures at different regions. An over-all increase in electron density is noticeable in the axolemma of the larger axons (*c* and *d*) as compared to the Schwann cell plasma membranes of the same fibers and to the axolemma of the smaller axons (*a* and *b*).

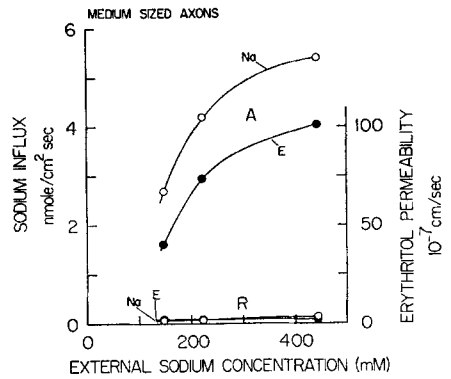

FIGURE 10. Sodium influx (*Na*) and erythritol permeability (*E*) at rest (*R*) and during activity (*A*), represented as functions of external sodium concentrations. The decline of the resting sodium influx is linear over this concentration range (see reference 1). Experiments carried out in medium sized axons. Temperature, 21–23°C. Values calculated from data in Tables V and VI of reference 1.

Since the nonelectrolyte penetration during activity approaches the resting value when the sodium concentration in the medium approaches zero, this may be considered to indicate that $L_{nn}X_n$ represents the resting value of the nonelectrolyte penetration. Therefore, $(L_{ne}/L_{ee})J_e$ should represent the nonelectrolyte entry due to the coupling between sodium and nonelectrolyte. In the resting axon this latter term is negligible, as follows from the experiments in which nonelectrolyte permeability was measured in medium sized axons at rest at different external sodium concentrations. The direct coefficient, L_{ee}, does not appear to be a function of axon diameter, no relationship having been observed between electrical parameters and nerve diameter. Therefore the decline in nonelectrolyte permeability during activity with axon diameter should be due to changes in the cross-coefficient, L_{ne}.

The nonelectrolyte-sodium coupling could be mediated by water movement. In such case the equations should be extended to include the water fluxes.

The coupling, previously proposed to explain the results in medium sized axons (see reference 1), does not imply that ions and molecules move through the same pathways; i.e., a transient osmotic gradient produced by the influx of sodium during activity could drag nonelectrolytes and water by the same and/or by different routes. It would be extremely interesting to demonstrate that nonelectrolytes can pass through ionic channels.

Our thanks are due to Dr. Margarita Blei for her collaboration; to Drs. F. J. Brinley, Flor V. Barnola, and M. Tamers for reading the manuscript; to Messrs. J. Aristimuño, J. Mora, J. L. Bigorra, and E. Peláez for their technical assistance; and to Miss María A. Zapata and Mrs. C. García for the preparation of this manuscript.

Received for publication 12 November 1970.

REFERENCES

1. VILLEGAS, R., G. M. VILLEGAS, M. BLEI, F. C. HERRERA, and J. VILLEGAS. 1966. Nonelectrolyte penetration and sodium fluxes through the axolemma of resting and stimulated medium sized axons of the squid *Doryteuthis plei*. *J. Gen. Physiol.* **50**:43.

2. MULLINS, L. J. 1966. Ion and molecule fluxes in squid axons. *Ann. N. Y. Acad. Sci.* **137**:830.
3. HIDALGO, C., and R. LATORRE. 1970. Effect of stimulation and hyperpolarization on non-electrolyte and sodium permeability in perfused axons of squid. *J. Physiol. (London).* **211**:193.
4. VILLEGAS, G. M., and R. VILLEGAS. 1968. Ultrastructural studies of the squid nerve fibers. *J. Gen. Physiol.* **51** (5, Pt. 2): 44s.
5. VILLEGAS, R., L. VILLEGAS, M. GIMENEZ, and G. M. VILLEGAS. 1963. Schwann cell and axon electrical potential differences. Squid nerve structure and excitable membrane location. *J. Gen. Physiol.* **46**:1047.
6. HODGKIN, A. L., and B. KATZ. 1949. The effect of sodium ions on the electrical activity of the giant axon of the squid. *J. Physiol. (London).* **108**:37.
7. VILLEGAS, R., I. B. BRUZUAL, and G. M. VILLEGAS. 1968. Equivalent pore radius of the axolemma of resting and stimulated squid axons. *J. Gen. Physiol.* **51** (5, Pt. 2): 81s.
8. KEYNES, R. D. 1951. The ionic movements during nervous activity. *J Physiol. (London).* **114**:119.
9. SHANES, A. M., and M. D. BERMAN. 1955. Kinetics of ion movements in the squid giant axon. *J. Gen. Physiol.* **39**:279.
10. BRINLEY, F. J., and L. J. MULLINS. 1965. Ion fluxes and transference numbers in squid axons. *J. Neurophysiol.* **28**:526.
11. KEYNES, R. D., and P. R. LEWIS. 1961. The sodium and potassium content of cephalopod nerve fibers. *J. Physiol. (London).* **114**:151.
12. ELFVIN, L. G. 1961. Electron microscopic investigation of the plasma membrane and myelin sheath of autonomic nerve fibers in the cat. *J. Ultrastruct. Res.* **5**:388.
13. VILLEGAS, R., C. CAPUTO, and L. VILLEGAS. 1962. Diffusion barriers in the squid nerve fiber. The axolemma and the Schwann layer. *J. Gen. Physiol.* **46**:245.